# NUMERICAL SOLUTION OF REACTING LAMINAR FLOW HEAT AND MASS TRANSFER IN DUCTS OF ARBITRARY CROSS-SECTIONS FOR NEWTONIAN AND NON-NEWTONIAN FLUIDS

***M. A. Isazadeh***

*Department of Chemical Engineering, University of Petroleum Industry*
*Ahwaz, Iran*

**(Received: March 27, 2002- Accepted in Revised Form: October 7, 2002)**

**Abstract** This study is concerned with the numerical analysis, formulation, programming and computation of steady, 3D conservation equations of reacting laminar flow heat and mass transfer in ducts of arbitrary cross-sections. The non-orthogonal boundary-fitted coordinate transformation method is applied to the Cartesian form of overall-continuity, momenta, energy and species-continuity equations, parabolized in the axial direction. The boundary conditions are also transformed accordingly. Applying a novel feature of the solution procedure, the contravariant velocity components are introduced into the transformed equations while the physical Cartesian velocity components are retained as dependent variables of the velocity field in the equations. The transformed equations are integrated over 3D control-volumes, followed by differencing the convective and diffusive terms by upwind and central-difference schemes respectively. A modified version of the SIMPLER algorithm is introduced in the solution procedure and a line-by-line TDMA algorithm is employed for the solution of discretization equations. A computer-programe is developed for the generation of non-orthogonal grids corresponding to Patankar's B-type arrangement in the transformed plane. A general computer programme in FORTRAN is developed for the solution of flow, heat and mass transfer problems for laminar reacting flows in straight ducts of arbitrary cross-sections. The model and computer codes are validated by theoretical, experimental and numerical results from various sources. The computer programs are employed for studies in the analysis of hydrodynamics and heat transfer in the entrance regions of ducts of arbitrary cross-sections for Newtonian and non-Newtonian fluids and ultimately for simulation of production of polystyrene in arbitrary cross-sectional duct reactors.

**Key Words** Boundary-Fitted Coordinates, Arbitrary Cross-Sectional Ducts, Reacting Flow, Heat and Mass Transfer, Non-Newtonian Fluids

**چکیده** ایـن مطالعه در رابطه با آنالیز عددی، فرمول بندی، برنامه نویسی و محاسبات انتقال حرارت و انتقال جـرم بـرای معادلات سه بعدی بقا در جریان آرام در حال واکنش در مجراهای با سطوح مقطع دلخواه می‌باشد. روش انتقال مختصات غیرمتعامد دربرگیرنده حدود اشکال هندسی برای شکل کارتزین معادلات پیوستگی کلی، مومنـتوم، انـرژی و پیوستگی جزئی که در جهت محوری پارابولیزه شده باشد، بکار برده می‌شود. شرایط مرزی نـیز بهمیـن طـریق انـتقال مـی‌یابند. با بکار بردن یک شیوه جدید راه حل، مولفه‌های سرعت کونتراواریانت در معادلات انتقال یافته داخل می‌گردند. در شرایطی که مولفه‌های سرعت فیزیکی کارتزین بعنوان متغیرهای وابسته در مـیدان سـرعت در معـادلات نگهـداری مـی‌شـوند. معـادلات انـتقال یافـته روی حجمهای کنترل سه بعدی انـتگرالگـیری و متعاقباً با بکار بردن روش upwind برای جملات کنوکسیون و روش central-difference برای جمـلات دیفـیوژن توزیـع گسسـته discretize مـی‌شـوند. شـکل جدیـد الگوریـتم Simpler در حـل معادلات discretize شده بکار برده می‌شود در حالی که این معادلات با الگوریتم TDMA بطور خط به خط حل می‌شوند. یـک برنامه رایانه ای برای ساختن شبکه های غیرمتعامد بر مبنای نوع B روش Patankar در صفحه انتقال یافته و همچنیـن یـک برنامه کلی رایانه‌ای برای حل مسائل جریان انتقال حرارت و انتقال جرم در جریانهای آرام در حـال واکـنش در مجراهای مستقیم با سطوح مقطع دلخواه ایجاد شده است. صحت مدل ریزی ریاضی و برنامه هـای رایانـه ای بـا نـتایج نظـری، تجربی و عددی از منابع مختلف اثبات شده است. برنامه های رایانه ای برای مطالعه و تجزیه و تحلیل هیدرودینامیکی و انتقال حرارت در قسمتهای ورودی مجراهای با سطوح مقطع دلخواه در سـیالات نیوتنـی و غیر نیوتنی و نیز از نظر انتقال جرم برای مشابه سازی تولید پلی استایرن در راکتورهای با سطوح مقطع دلخواه بکار شده است.

## 1. INTRODUCTION

The subjects in transport phenomena are modeled by nonlinear-coupled partial-differential equations. These equations can be solved by several approximate solution methods for special cases

such as asymptotic-expansion and perturbation methods ,collocation and integral methods, finite-difference, finite-volume, and finite-element methods [1]. In general, finite-difference, finite-volume and finite-element discretization techniques have been the most successful methods the use of which, however ,requires discretizing the entire domain employing a mesh or a grid network.

The finite element method has been concerned with the treatment of irregular boundaries since its beginning, however, this method requires excessive amount of computational time and storage [2].

In finite difference methods a convenient choice for a grid network is composed of rectangles. The application of the method is therefore suitable to domains such as rectangular shapes whose boundaries coincide with the computational grid points. In earlier studies whenever the finite-difference method was applied to irregular-shape domains, special interpolation schemes were employed at the boundaries for discretization of the boundary conditions. However, this method can lead to large errors. In any boundary value problem, the boundary conditions exert a strong influence on the solution of the interior of the domain, so that greater accuracy is required in the representation of the difference equations at the boundaries than what is obtained by interpolation.

The inadequacy of the interpolation methods and the fact that an accurate expression of the boundary conditions is best accomplished if the boundaries coincide with some coordinate lines, brought about the development of coordinate transformation of the physical domain i.e. Cartesian coordinates to boundary-fitted curvilinear coordinates such that all the boundaries match the coordinate lines and the need to interpolate the boundary conditions is eliminated [3-7]. Appropriate transformation relations thus transform the partial differential equations from the Cartesian coordinates into the new coordinate system. The boundary conditions are similarly transformed without the need to use interpolation techniques. The transformed plane is simply a rectangular domain. The transformed-equations and the boundary conditions are discretized over this plane and the discretized equations are conveniently solved by similar methods in Cartesian space. It has been shown that the partial differential equations do not change their type, i.e. elliptic, parabolic or hyperbolic upon transformation.

A review of some of the related developments in the numerical methods for the solution of momentum equations reveals the elegant features of the numerical procedure applied in this work. In general, coupling between the momentum and mass conservation equations is often the major cause of the slow convergence of the iterative solution methods. Caretto et al. [8] applied a numerical method to the solution of the momentum equations, which involved an implicit simultaneous solution of coupled nonlinear difference equations without linearization or decoupling. The solution procedure was, however, a point-by-point iterative method due to which slow convergence is inevitable. The method of Patankar and Spalding [9] involved linearization and decoupling of the equations. In their method, the non-linear terms (the product terms) of the momentum equations are handled by setting the value of velocities in these terms the same as their values at the previous axial step. The axial momentum equation is treated separately from the transverse momentum equations, which are decoupled by assuming a pressure-field in the transverse direction. In the computations of transverse velocities, corrections are made for tentative transverse velocities and pressure field by iteratively solving a Poisson like equation for the pressure-correction. The method proposed by Briley [10] requires two Poisson like equations to solve, one for a velocity potential for velocity corrections and the other for the pressure field. The method of Patankar and Spalding [9] developed later brought about the SIMPLE and SIMPLER algorithms [11]. The SIMPLE and SIMPLER algorithms have been already applied to solve problems using the non-orthogonal boundary fitted coordinate transformation system. For example, Hadjisophocleous et al. [12], Shyy et al. [13] and Braaten et al. [14] employed the SIMPLE algorithm in their analysis for non-orthogonal systems. Maliska [15, 16] applied a mixed scheme comprising of the SIMPLE and SIMPLER algorithms. In the present work, the SIMPLER algorithm is further developed for the solution of the power-law non-Newtonian fluid problems.

## 2. THE MATHEMATICAL MODELLING

The strongly conservative form of the conservation equations in Cartesian coordinates are employed [17] in this work. The conservative form enhances the subsequent treatment of the equations for numerical solution. The rheology of many purely viscous non-Newtonian fluids is adequately expressed by the power-law model [18,19] for which the corresponding constitutive equation is expressed as follows:

$$\tau_{ij} = -\mu \left| \sqrt{\frac{1}{2}(\Delta_{ij} : \Delta_{ij})} \right|^{n-1} \Delta_{ij} \tag{1}$$

in which

$$\frac{1}{2}(\Delta_{ij} : \Delta_{ij}) = 2\left[\left(\frac{\partial u}{\partial x}\right)^2 + \left(\frac{\partial v}{\partial y}\right)^2 + \left(\frac{\partial w}{\partial z}\right)^2\right] + \left(\frac{\partial u}{\partial y} + \frac{\partial v}{\partial x}\right)^2 + \left(\frac{\partial w}{\partial y} + \frac{\partial v}{\partial z}\right)^2 + \left(\frac{\partial u}{\partial z} + \frac{\partial w}{\partial x}\right)^2 \tag{2}$$

The diffusion terms are neglected in the axial direction in the conservation equations and the equations are parabolized in this direction. The free-convection effect (buoyancy term) is introduced in the "y" momentum equation while the pressure-field is modified [21, 22]. The heat of reaction and the viscous dissipation effects are considered in the energy equation. The Arrhenius model or any empirically obtained rate law may be employed for any reaction under study. Variable physical properties may be considered except for specific heat, which is nearly constant for liquids within some specified temperature ranges.

## 3. THE PARABOLIZED GOVERNING EQUATIONS IN CARTESIAN COORDINATES

### The Overall Continuity Equation

$$\frac{\partial(\rho u)}{\partial x} + \frac{\partial(\rho v)}{\partial y} + \frac{\partial(\rho w)}{\partial z} = 0 \tag{3}$$

### The Momentum Equations

**x- Component**

$$\frac{\partial(\rho u^2)}{\partial x} + \frac{\partial(\rho vu)}{\partial y} + \frac{\partial(\rho wu)}{\partial z} = -\frac{\partial P}{\partial x} - \left(\frac{\partial \tau_{xx}}{\partial x} + \frac{\partial \tau_{yx}}{\partial y}\right) \tag{4}$$

**y- Component**

$$\frac{\partial(\rho uv)}{\partial x} + \frac{\partial(\rho v^2)}{\partial y} + \frac{\partial(\rho wv)}{\partial z} = -\frac{\partial P}{\partial y} - \left(\frac{\partial \tau_{xy}}{\partial x} + \frac{\partial \tau_{yy}}{\partial y}\right) - (\rho - \rho_a)g \tag{5}$$

**z- Component**

$$\frac{\partial(\rho\rho uw}{\partial x} + \frac{\partial(\rho\rho vw}{\partial y} + \frac{\partial(\rho\rho^{\ 2})}{\partial z} = -\frac{\partial \overline{P}}{\partial z} - \left(\frac{\partial \tau_{xz}}{\partial x} + \frac{\partial \tau_{yz}}{\partial y}\right) \tag{6}$$

### The Energy Equation

$$\frac{\partial}{\partial x}(\rho C_P T u) + \frac{\partial}{\partial y}(\rho C_P T v) + \frac{\partial}{\partial z}(\rho C_P T w) = \frac{\partial}{\partial x}(k\frac{\partial T}{\partial x}) + \frac{\partial}{\partial y}(k\frac{\partial T}{\partial y}) + M.\Phi_v + (-\Delta H)R_A \tag{7}$$

### The Reactant Continuity Equation

$$\frac{\partial}{\partial x}(\rho m_A u) + \frac{\partial}{\partial y}(\rho m_A v) + \frac{\partial}{\partial z}(\rho m_A w) = \frac{\partial}{\partial x}(\rho D_A \frac{\partial m_A}{\partial x}) + \frac{\partial}{\partial y}(\rho D_A \frac{\partial m_A}{\partial y}) - R_A \tag{8}$$

The pressure, P in the above equations is dynamic-pressure due to the introduction of buoyancy term in the "y" momentum equation. In cases of negligible buoyancy effect, P would be the total pressure defined as hydrostatic plus dynamic pressures.

## The Boundary Conditions

**Inlet (@z =0)**

**Axial Velocity** A uniform entrance velocity profile is specified at inlet:

$$w = w_{inlet} \tag{9}$$

**Transverse Velocities** It is assumed that, there is no secondary flow at inlet:

$$u = 0, v = 0 \tag{10}$$

**Temperature** A uniform temperature-profile is specified at inlet:

$$T = T_{inlet} \tag{11}$$

**Reactant Weight Fraction** For an unconverted reactant at inlet:

$$m = 1 \tag{12}$$

## Walls of the Duct

**Axial Velocity** No slip-condition is assumed on the walls of the duct

$$w = 0 \tag{13}$$

**Transverse Velocities**

$$u = 0, v = 0 \tag{14}$$

**Temperature** For a constant wall- temperature:

$$T = T_{wall} \tag{15}$$

**Reactant Weight-Fraction** The material does not move through the wall

$$\frac{\partial m}{\partial n} = 0 \tag{16}$$

**Outflow Condition (@z = L)** The complete conservation equations are elliptic; hence the geometrical domain under consideration must be closed; that is, for duct flow, the downstream boundary conditions have to be specified. However for the parabolized governing equations used here no downstream boundary conditions are required.

## 4. THE NUMERICAL SOLUTION

**The Orthogonal and Non-Orthogonal Coordinate Systems** The curvilinear boundary-fitted mesh generated over the physical domain, may be either orthogonal or non-orthogonal. The generation of orthogonal meshes is generally time-consuming [15]. In addition, the concentration of the grid lines in certain regions of the domain is not conveniently handled when using orthogonal methods. The use of non-orthogonal systems has the disadvantage that the transformed governing equations become somewhat more complex because of the presence of the non-orthogonal terms. Also the finite-difference equations for pressure-correction involve 9 discrete-points versus 5 discrete points for orthogonal systems [15, 16]. The use of non-orthogonal coordinates versus orthogonal system has the advantage of getting rid of the generation of orthogonal grids at certain locations which are difficult or impossible to make. The boundary-fitted method involves the following two tasks for the solution of PDE's:

i. method for generating the coordinate system or grid network.
ii. method to model the governing equations in the transformed domain.

A number of studies have appeared in literature on the use of the non-orthogonal numerical solution schemes. For example Hadjisophocleous et al. [12] applied a non-orthogonal numerical method for the prediction of transient natural

convection in enclosures of arbitrary geometry. Shyy, et al. [13] and Braaten, et al. [14] applied a non-orthogonal numerical scheme using boundary-fitted coordinates for numerical solution of a recirculation flow problem. Maliska [16] developed a numerical model using non-orthogonal grids for the solution of three-dimensional fluid-flow problems in irregular geometries. This method uses a novel grid layout, which promotes numerical stability and convergence for the system of equations. Maliska's method is adopted here to be applied to the present analysis considering also any developments required.

**Curvilinear Transformation** A transformation is defined between a physical region "D" of any arbitrary shape and a transformed region of "D*" of rectangular-shape. In the physical-region, the Cartesian coordinates x and y are the independent variables and the curvilinear coordinates ξ and η are the dependent variables. In the transformed region, the coordinates ξ and η are the independent variables and x and y are the dependent variables. There exists a one to one correspondence between the coordinates in the physical-region and the transformed-region.

The general transformation relation from the physical-plane (x, y) to the transformed- plane (ξ, η) are given by [3-7]:

$$\begin{aligned} \xi &= \xi\,(x,\,y) \\ \eta &= \eta\,(x,\,y) \end{aligned} \tag{17}$$

The inverse transformation of Equation 17 (if exists) is:

$$\begin{aligned} x &= x(\xi,\eta) \\ y &= y(\xi,\eta) \end{aligned} \tag{18}$$

The Jacobian determinant or Jacobian simply, is then

$$J = J\left[\frac{(x,y)}{(\xi,\eta)}\right] = x_\xi y_\eta - x_\eta y_\xi \neq 0 \tag{19}$$

where

$$x_\xi = \frac{\partial x}{\partial \xi}; y_\eta = \frac{\partial y}{\partial \eta}; etc. \tag{20}$$

one can readily show that:

$$\begin{aligned} \xi_x &= \frac{y_\eta}{J} \qquad \eta_x = -\frac{y_\xi}{J} \\ \xi_y &= -\frac{x_\eta}{J} \quad \eta_y = \frac{x_\xi}{J} \end{aligned} \tag{21}$$

Partial derivatives are transformed using the following relations:

$$\begin{aligned} f_x &= \frac{1}{J}\left[y_\eta\, f_\xi - y_\xi\, f_\eta\right] \\ f_y &= \frac{1}{J}\left[-\,x_\eta\, f_\xi + x_\xi\, f_\eta\right] \end{aligned} \tag{22}$$

Higher order derivatives are obtained by repeated application of Equation 22.

**Numerical Grid Generation** Consider a simply connected region, the boundary of which is specified at discrete-points ($x_b$, $y_b$). The simplest elliptic system to choose is to use Laplace equation and to find ξ, η so that a system of Laplace equations is satisfied in the physical plane, that is:

$$\begin{aligned} \xi_{xx} + \xi_{yy} &= 0 \\ \eta_{xx} + \eta_{yy} &= 0 \end{aligned} \tag{23}$$

subject to Dirichlet boundary conditions.

Since it is desired to perform all the numerical computations on the uniform rectangular transformed plane, the dependent and independent variables in the above equations must be interchanged. This results in:

$$\begin{aligned} \alpha x_{\xi\xi} - 2\beta x_{\xi\eta} + \gamma x_{\eta\eta} &= 0 \\ \alpha y_{\xi\xi} - 2\beta y_{\xi\eta} + \gamma y_{\eta\eta} &= 0 \end{aligned} \tag{24}$$

The coupling coefficients in the above-equations are:

$$\alpha = x_\eta^2 + y_\eta^2$$
$$\beta = x_\xi x_\eta + y_\xi y_\eta \quad (25)$$
$$\gamma = x_\xi^2 + y_\xi^2$$

Equation 24 can be solved by a finite-difference method using second-order central difference approximation of derivatives and applying the SOR (successive over-relaxation) method. The discrete values of (x, y) at the corresponding (ξ, η) points are then determined. The grid generation method described in this section is employed to develop a B-type grid generation computer program required in this work [11].

## 5. TRANSFORMATION OF THE GOVERNING EQUATIONS

The governing partial-differential equations and the respective boundary conditions must be transformed to the boundary-fitted curvilinear coordinates in order to be solved in the transformed plane. The problem of solving the governing-equations on a complex physical domain is therefore changed to the solution of the transformed-equations on a uniform grid of rectangular shape in the transformed plane. In general, the transformation operation generates additional terms in the governing equations so that these equations become more complicated upon transformation.

For the transformation of the governing equations, one has to first decide upon the de pendent variables in the transformed-plane for the velocity components, which could be either the physical Cartesian velocities, or the contravariant velocity components. The contravariant velocities are related to the physical Cartesian components by the following relationships:

$$U = y_\eta u - x_\eta v$$
$$V = x_\xi v - y_\xi u \quad (26)$$
$$W = Jw$$

Use of contravariant velocities - as the dependent variables - leads to a complex transformation in which the physical interpretation of the transformed equations is also very difficult. Retaining the physical Cartesian velocities as the dependent variables in the transformation of the equations has the advantage that very complex transformed equations are avoided. Also the equations preserve their conservative form after transformation, which is a desired feature in the physical interpretation of the equations and in the convenience of formulation of discretization equations.

The dependent variables for velocity components selected in this analysis are the physical- Cartesian velocities; however, both the Cartesian and the contravariant velocities take part in the structure of the transformed equations and in the solution procedure. The transformed forms of the parabolized governing equations are as follows:

### The Overall Continuity Equation

$$\frac{\partial}{\partial\xi}(\rho U) + \frac{\partial}{\partial\eta}(\rho V) + \frac{\partial}{\partial\sigma}(\rho W) = 0 \quad (27)$$

### The Momentum Equations

**x-Component**

$$\frac{\partial}{\partial\xi}(\rho uU) + \frac{\partial}{\partial\eta}(\rho uV) + \frac{\partial}{\partial\sigma}(\rho uW) =$$
$$-\frac{\partial}{\partial\xi}[y_\eta(\hat{\tau}_{xx}) - x_\eta(\hat{\tau}_{yx})] -$$
$$\frac{\partial}{\partial\eta}[x_\xi(\hat{\tau}_{yx}) - y_\xi(\hat{\tau}_{xx})] - [y_\eta P_\xi - y_\xi P_\eta] \quad (28)$$

**y-Component**

$$\frac{\partial}{\partial\xi}(\rho vU) + \frac{\partial}{\partial\eta}(\rho vV) + \frac{\partial}{\partial\sigma}(\rho vW) =$$
$$-\frac{\partial}{\partial\xi}[y_\eta(\hat{\tau}_{xy}) - x_\eta(\hat{\tau}_{yy})] -$$
$$\frac{\partial}{\partial\eta}[x_\xi(\hat{\tau}_{yy}) - y_\xi(\hat{\tau}_{xy})] - \quad (29)$$
$$[x_\xi P_\eta - x_\eta P_\xi] - J(\rho - \rho_\alpha)g$$

**z- Component**

$$\frac{\partial}{\partial\xi}(\rho\rho wU+\frac{\partial}{\partial\eta}(\rho\rho wV+\frac{\partial}{\partial\sigma}(\rho\rho wW=$$
$$-\frac{\partial}{\partial\xi}[y_\eta(\hat{\tau}_{xz})-x_\eta(\hat{\tau}_{yz})]-$$
$$\frac{\partial}{\partial\eta}[x_\xi(\hat{\tau}_{yz})-y_\xi(\hat{\tau}_{xz})]-J\frac{d\overline{P}}{d\sigma} \quad (30)$$

## The Energy Equation

$$\frac{\partial}{\partial\xi}(\rho C_pTU)+\frac{\partial}{\partial\eta}(\rho C_pTV)+\frac{\partial}{\partial\sigma}(\rho C_pTW)=$$
$$\frac{\partial}{\partial\xi}\left[\frac{\alpha}{J}kT_\xi-\frac{\beta}{J}kT_\eta\right]$$
$$+\frac{\partial}{\partial\eta}\left[\frac{\gamma}{J}kT_\eta-\frac{\beta}{J}kT_\xi\right]+J\hat{M}\hat{\Phi}_v+J(-\Delta H)\hat{R}_A \quad (31)$$

## The Reactant Continuity Equation

$$\frac{\partial}{\partial\xi}(\rho m_AU)+\frac{\partial}{\partial\eta}(\rho m_AV)+\frac{\partial}{\partial\sigma}(\rho m_AW)=$$
$$\frac{\partial}{\partial\xi}\left[\frac{\rho D_A}{J}\alpha m_\xi-\frac{\rho D_A}{J}\beta m_\eta\right] \quad (32)$$
$$+\frac{\partial}{\partial\eta}\left[\frac{\rho D_A}{J}\gamma m_\eta-\frac{\rho D_A}{J}\beta m_\xi\right]-J\hat{R}_A$$

where $m\equiv m_A$ for the derivatives.

The boundary conditions are also transformed. The transformed components of the stress tensor, expressed by the power-law constitutive equation, are substituted in the transformed governing equations, which are then expanded to their ultimate form before being used for discretization. It is to be noted that the source term in the transformed energy equation is composed of the viscous dissipation and heat of reaction terms, while the source term in the transformed reactant continuity equation involves the rate of reactant consumption due to chemical reaction.

## 6. DISCRETIZATION OF TRANSFORMED EQUATIONS

**The Grid Configuration Adopted** For a non-orthogonal grid system, the best choice is a classical staggered-grid in which both components of "u" and "v" velocities are used coincidentally at the same location with the contravariant-velocities normal and parallel to the faces of the cell [16]. This configuration involves one difficulty, which can be solved by an interpolation scheme. Due to the fact that one of the contravariant velocities (parallel components) do not enter to satisfy the overall continuity equation, the "u" and "v" values can depart considerably from their realistic values during the iteration process. The values of these velocities can, however, produce normal components of the contravariant velocities, which would satisfy the mass balance equation while the parallel components of the contravariant velocities remain free to assume unrealistic values. The solution to this difficulty is to enforce somehow the continuity equation to also hold for the parallel components of the contravariant velocities. Thus the parallel components of the contravariant velocities are obtained by interpolation from the normal components of the contravariant velocities, which do satisfy the mass conservation.

**The Discretization Method** The transformed governing equations are discretized using the method known as the "control-volume" finite difference approach [11]. Applying this method, the calculation domain is divided into a number of control volumes such that there is one control-volume surrounding each grid-point. The differential equations are integrated over each control-volume. For 3D problems, triple integrals are involved. In the formulation of the discretization equations, the upwind difference scheme is applied to the convective terms and the central difference approximation to the diffusion terms. The fact that the flow field must satisfy the mass conservation equation provides some simplification to the discretized governing equations combined with the discretized overall continuity equation. Finally, each equation is cast into the general discretization form, that is, an algebraic relation connecting values of the dependent variable for a group of grid points,

bearing their respective coefficients. For each nodal point P, four adjacent control volumes surrounding the interfacial points (e n w and s) are considered over which the transformed transverse momentum equations are integrated and discretized. Thus, four pairs of discretization relations for u and v velocities, namely, ($n_e$, $v_e$), ($u_n$, $v_n$), ($u_w$, $v_w$) and ($u_s$, $v_s$) are obtained. Meanwhile, the transformed equations for axial momentum, energy and reactant continuity are integrated over the main control volume enclosing the nodal point P from which the discretization equations for $w_p$, $h_P$ and $m_P$ are obtained. The list of discretization equations is as follows:

$$u_e : AP_e^u u_e = \sum A_{(nb)_e}^u u_{(nb)_e} + B_e^u - \left\{ \begin{array}{l} \frac{P_E - P_P}{\Delta\xi} y_{\eta e} - \\ \frac{P_N + P_{NE} - P_S - P_{SE}}{4\Delta\eta} y_{\xi e} \end{array} \right\} \Delta V \quad (33)$$

$$v_e : AP_e^v v_e = \sum A_{(nb)_e}^v v_{(nb)_e} + B_e^v - \left\{ \begin{array}{l} \frac{P_N + P_{NE} - P_S - P_{SE}}{4\Delta\eta} x_{\xi e} - \\ \frac{P_E - P_P}{\Delta\xi} x_{\eta e} \end{array} \right\} \Delta V \quad (34)$$

$$u_n : AP_n^u u_n = \sum A_{(nb)_n}^u u_{(nb)_n} + B_n^u - \left\{ \begin{array}{l} \frac{P_{NE} + P_E - P_W - P_{NW}}{4\Delta\xi} y_{\eta n} - \\ \frac{P_N - P_P}{\Delta\eta} y_{\xi n} \end{array} \right\} \Delta V \quad (35)$$

$$v_n : AP_n^v v_n = \sum A_{(nb)_n}^v v_{(nb)_n} + B_n^v - \left\{ \begin{array}{l} \frac{P_N - P_P}{\Delta\eta} x_{\xi n} - \\ \frac{P_{NE} + P_E - P_W - P_{NW}}{4\Delta\xi} x_{\eta n} \end{array} \right\} \Delta V \quad (36)$$

$$u_w : AP_w^u u_w = \sum A_{(nb)_w}^u u_{(nb)_w} + B_w^u - \left\{ \begin{array}{l} \frac{P_P - P_W}{\Delta\xi} y_{\eta w} - \\ \frac{P_N + P_{NW} - P_S - P_{SW}}{4\Delta\eta} y_{\xi w} \end{array} \right\} \Delta V \quad (37)$$

$$v_w : AP_w^v v_w = \sum A_{(nb)_w}^v v_{(nb)_w} + B_w^v - \left\{ \begin{array}{l} \frac{P_N + P_{NW} - P_S - P_{SW}}{4\Delta\eta} x_{\xi w} \\ - \frac{P_P - P_W}{\Delta\xi} x_{\eta w} \end{array} \right\} \Delta V \quad (38)$$

$$u_s : AP_s^u u_s = \sum A_{(nb)_s}^u u_{(nb)_s} + B_s^u - \left\{ \begin{array}{l} \frac{P_E + P_{SE} - P_W - P_{SW}}{4\Delta\xi} y_{\eta s} \\ - \frac{P_P - P_S}{\Delta\eta} y_{\xi s} \end{array} \right\} \Delta V \quad (39)$$

$$v_s : AP_s^v v_s = \sum A_{(nb)_s}^v v_{(nb)_s} + B_s^v - \left\{ \begin{array}{l} \frac{P_P - P_S}{\Delta\eta} x_{\xi s} \\ - \frac{P_E + P_{SE} - P_W - P_{SW}}{4\Delta\xi} x_{\eta s} \end{array} \right\} \Delta V \quad (40)$$

$$w_P : AP_P^w . w_P = \sum A_{(nb)P}^w . w_{(nb)P} + B_P^w - J_P \left[ \frac{\Delta \overline{P}}{\Delta \sigma} \right] \Delta V \quad (41)$$

$$h_P : AP_P^h . h_P = \sum A_{(nb)P}^h . h_{(nb)P} + B_P^h \quad (42)$$

$$m_P : AP_P^m . m_P = \sum A_{(nb)P}^m . m_{(nb)P} + B_P^m \quad (43)$$

Note that there exists the following relationship for the coefficients of each discretization equation:

$$AP = AE + AN + AW + AS + AU \quad (44)$$

Introducing source-term linearization for energy and species-continuity equations:

$$AP = AE + AN + AW + AS + AU - SP.\Delta V \tag{45}$$

**Location of the Control-Volume Faces** For the proper location of the control-volume faces, the B-type grid or practice-B [11] is employed here. In this arrangement, one draws first the control-volume boundaries and then places a grid-point at the geometric center of each control-volume through which the main grid lines are drawn. If the grid is designed this way, then the entire calculation domain would be covered with regular control-volumes.

**The Solution Method of the Discretization Equations** The discretization equations are algebraic equations and are solved by a line-by-line tridiagonal matrix (TDMA) algorithm. Introducing a relaxation-factor to the discretization equations one may enhance the convergence of the iterative solution. With the line-by-line method, use of over relaxation is uncommon while underrelaxation is often used to avoid divergence in the iterative solution of the equation. The general discretization equation in which relaxation factor is introduced is as follows:

$$\begin{aligned} &AP(I,J)\phi(I,J) = \\ &\sum A_{(nb)}(I,J)\phi_{(nb)}(I,J) + B(I,J) + \\ &(1-\alpha)AP(I,J)\phi(I,J) - L[\hat{P}_P]\Delta V \end{aligned} \tag{46}$$

**Pressure-Velocity Coupling in the Transverse Direction** The SIMPLER algorithm is modified for non-orthogonal system and power-law non-Newtonian fluids in this work. The coefficients of the "u" and "v" momentum equations are computed using the best available velocities. A Poisson-like equation for pressure using pseudo velocities is solved to obtain a tentative pressure-field, P*, which is used to solve the "u" and "v" momentum equations to obtain the starred-velocities $u^*$ and $v^*$. These velocities do not, in general, conserve mass. The corresponding values of $U^*$ and $V^*$ are obtained by substituting $u^*$ and $v^*$ in the following relations:

$$\begin{aligned} U^* &= y_\eta u^* - x_\eta v^* \\ V^* &= x_\xi v^* - y_\xi u^* \end{aligned} \tag{47}$$

These velocities must be corrected by $U - U^*$ and $V - V^*$ respectively, to obtain "$U$" and "$V$" velocities which do conserve mass. The above changes are related to the corresponding required changes in the "u" and "v" velocities as follows:

$$\begin{aligned} U - U^* &= y_\eta (u - u^*) - x_\eta (v - v^*) \\ V - V^* &= x_\xi (v - v^*) - y_\xi (u - u^*) \end{aligned} \tag{48}$$

Estimates of change in "$u$" and "$v$" that result from change in "$P$" are:

$$u_e - u_e^* = -\frac{\Delta V}{A_e^u}\left\{\begin{aligned} &\frac{P'_E - P'_P}{\Delta\xi}(y_\eta)_e - \\ &\frac{P'_N + P'_{NE} - P'_S - P'_{SE}}{4\Delta\eta}(y_\xi)_e \end{aligned}\right\}$$

$$v_e - v_e^* = -\frac{\Delta V}{A_e^v}\left\{\begin{aligned} &\frac{P'_N + P'_{NE} - P'_S - P'_{SE}}{4\Delta\eta}(x_\xi)_e - \\ &\frac{P'_E - P'_P}{\Delta\xi}(x_\eta)_e \end{aligned}\right\} \tag{49}$$

in which $P' = P - P^*$. Similar expressions are obtained for $u_n - u_n^*$, $v_n - v_n^*$, $u_w - u_w^*$, $v_w - v_w^*$, $u_s - u_s^*$ and $v_s - v_s^*$. The value of $P'$ is obtained from a Poisson-like pressure-correction equation derived in this work for the power-law non-Newtonian fluid in which the starred velocities are used. Once the $P'$ is known, the contravariant velocities which enter into the mass-balance ($U_e$, $U_w$, $V_s$, $V_n$) can be found from the Equation 48. The other contravariant velocities ($V_e$, $U_n$, $V_w$, $U_s$) are obtained by interpolation. The physical velocities "$u$" and "$v$" are obtained from the following

equations:

$$u = \frac{1}{J}\left[Ux_{\xi} + Vx_{\eta}\right]$$
$$v = \frac{1}{J}\left[Uy_{\xi} + Vy_{\eta}\right] \quad (50)$$

To obtain an equation for pressure correction, $P'$ one should substitute the velocity-correction (49) etc. in Equation 48 to obtain equations for "$U$" and "$V$" in terms of $U^*$, $V^*$ and $P'$ which when substituted in the overall continuity equation:

$$\frac{(\rho U)_e - (\rho U)_w}{\Delta\xi} + \frac{(\rho V)_n - (\rho V)_s}{\Delta\eta} + \frac{(\rho W)_D - (\rho W)_U}{\Delta\sigma} = 0 \quad (51)$$

results the following Poisson-like pressure-correction equation:

$$A_P P' = A_E P'_E + A_N P'_N + A_S P'_S + A_W P'_W + A_{NE} P'_{NE} + A_{SE} P'_{SE} + A_{NW} P'_{NW} + A_{SW} P'_{SW} + B \quad (52)$$

in which

$$A_P = A_E + A_N + A_W + A_S \quad (53)$$

also

$$A_{NE} + A_{NW} + A_{SW} + A_{SE} = 0 \quad (54)$$

Taking "$\rho$" constant in the above formulations (which enhances convergence) and using $\Delta\xi=\Delta\eta=1$ (for simplicity), the coefficients are obtained as follows:

$$A_p = \frac{\Delta\sigma y_{\eta e}^2}{AP_e^u} + \frac{\Delta\sigma x_{\eta e}^2}{AP_e^v} + \frac{\Delta\sigma y_{\eta w}^2}{AP_w^u} + \frac{\Delta\sigma x_{\eta w}^2}{AP_w^v} + \frac{\Delta\sigma y_{\xi n}^2}{AP_n^u} + \frac{\Delta\sigma x_{\xi n}^2}{AP_n^v} + \frac{\Delta\sigma x_{\xi s}^2}{AP_s^v} + \frac{\Delta\sigma y_{\xi s}^2}{AP_s^u} \quad (55)$$

$$A_E = \frac{\Delta\sigma y_{\eta e}^2}{AP_e^u} + \frac{\Delta\sigma x_{\eta e}^2}{AP_e^v} - \frac{\Delta\sigma x_{\xi n} x_{\eta n}}{4AP_n^v} - \frac{\Delta\sigma y_{\xi n} y_{\eta n}}{4AP_n^u} + \frac{\Delta\sigma x_{\xi s} x_{\eta s}}{4AP_s^v} + \frac{\Delta\sigma y_{\xi s} y_{\eta s}}{4AP_s^u} \quad (56)$$

$$A_N = -\frac{\Delta\sigma y_{\xi e} y_{\eta e}}{4AP_e^u} - \frac{\Delta\sigma x_{\xi e} x_{\eta e}}{4AP_e^v} + \frac{\Delta\sigma y_{\xi w} y_{\eta w}}{4AP_w^u} + \frac{\Delta\sigma x_{\xi w} x_{\eta w}}{4AP_w^v} + \frac{\Delta\sigma x_{\xi n}^2}{AP_n^v} + \frac{\Delta\sigma y_{\xi n}^2}{AP_n^u} \quad (57)$$

$$A_S = \frac{\Delta\sigma y_{\xi e} y_{\eta e}}{4AP_e^u} + \frac{\Delta\sigma x_{\xi e} x_{\eta e}}{4AP_e^v} - \frac{\Delta\sigma y_{\xi w} y_{\eta w}}{4AP_w^u} - \frac{\Delta\sigma x_{\xi w} x_{\eta w}}{4AP_w^v} + \frac{\Delta\sigma x_{\xi s}^2}{AP_s^v} + \frac{\Delta\sigma y_{\xi s}^2}{AP_s^u} \quad (58)$$

$$A_W = \frac{\Delta\sigma y_{\eta w}^2}{AP_w^u} + \frac{\Delta\sigma x_{\eta w}^2}{AP_w^v} + \frac{\Delta\sigma x_{\xi n} x_{\eta n}}{4AP_n^v} + \frac{\Delta\sigma y_{\xi n} y_{\eta n}}{4AP_n^u} - \frac{\Delta\sigma x_{\xi s} x_{\eta s}}{4AP_s^v} - \frac{\Delta\sigma y_{\xi s} y_{\eta s}}{4AP_s^u} \quad (59)$$

$$A_{NE} = -\frac{\Delta\sigma x_{\xi e} x_{\eta e}}{4AP_e^v} - \frac{\Delta\sigma y_{\xi e} y_{\eta e}}{4AP_e^u} - \frac{\Delta\sigma x_{\xi n} x_{\eta n}}{4AP_n^v} - \frac{\Delta\sigma y_{\xi n} y_{\eta n}}{4AP_n^u} \quad (60)$$

$$A_{SE} = +\frac{\Delta\sigma x_{\xi e} x_{\eta e}}{4AP_e^v} + \frac{\Delta\sigma y_{\xi e} y_{\eta e}}{4AP_e^u} + \frac{\Delta\sigma x_{\xi s} x_{\eta s}}{4AP_s^v} + \frac{\Delta\sigma y_{\xi s} y_{\eta s}}{4AP_s^u} \quad (61)$$

$$A_{NW} = \frac{\Delta\sigma x_{\xi w} x_{\eta w}}{4\,AP_w^{\,v}} + \frac{\Delta\sigma y_{\xi w} y_{\eta w}}{4\,AP_w^{\,u}} + \frac{\Delta\sigma x_{\xi n} x_{\eta n}}{4\,AP_n^{\,v}} + \frac{\Delta\sigma y_{\xi n} y_{\eta n}}{4\,AP_n^{\,u}} \quad (62)$$

$$A_{SW} = -\frac{\Delta\sigma x_{\xi w} x_{\eta w}}{4\,AP_w^{\,v}} - \frac{\Delta\sigma y_{\xi w} y_{\eta w}}{4\,AP_w^{\,u}} - \frac{\Delta\sigma x_{\xi s} x_{\eta s}}{4\,AP_s^{\,v}} - \frac{\Delta\sigma y_{\xi s} y_{\eta s}}{4\,AP_s^{\,u}} \quad (63)$$

$$B = (U_w^* - U_e^*) + (V_s^* - V_n^*) + \frac{W_U - W_D}{\Delta\sigma} \quad (64)$$

(for pressure-correction equation)

The Poisson-like pressure equation is similar to the equation for pressure-correction equation,

$$A_P P_P = A_E P_E + A_N P_N + A_S P_S + A_W P_W + A_{NE} P_{NE} + A_{SE} P_{SE} + A_{NW} P_{NW} + A_{SW} P_{Sw} + B \quad (65)$$

with the exception of the B term which is expressed in terms of pseudovelocities for the pressure equation.

$$B = (\hat{U}_w - \hat{U}_e) + (\hat{V}_s - \hat{V}_n) + \frac{W_U - W_D}{\Delta\sigma} \quad (66)$$

(for pressure equation)

**Pressure-Velocity Coupling in the Parabolic Direction** The method adopted here is that of Raithby/Schneider [23]. Primarily the momentum equation in the axial-direction is solved with the boundary condition using a guessed pressure-gradient $\left(\frac{\partial \hat{P}}{\partial\sigma}\right)$ to obtain a tentative axial-velocity $w_P^*$. The corresponding mass flow rate is

$$M^* = \sum_{allP} J\rho w^* \quad (67)$$

where "all P" denotes all the w-control volumes inside the duct walls. Defining two new variables:

$$Q = -\frac{\partial \overline{P}}{\partial\sigma} \text{ and } f_P = \frac{\partial w}{\partial Q} \quad (68)$$

The corrected pressure-gradient $\left(\frac{\partial \overline{P}}{\partial\sigma}\right)$ would be related to $\left(\frac{\partial \overline{P}}{\partial\sigma}\right)^*$ by

$$\Delta Q = -\left[\frac{\partial \overline{P}}{\partial\sigma} - \left(\frac{\partial \overline{P}}{\partial\sigma}\right)^*\right] \quad (69)$$

and the corrected axial-velocity would be related to $w_P^*$ by

$$w_P = w_P^* + f_P \Delta Q \quad (70)$$

where $f_P$ is obtained from the following discretization-equation using appropriate boundary- conditions:

$$A_P^w f_P = A_e^w f_E + A_w^w f_W + A_n^w f_N + A_s^w f_S + J_P \Delta V \quad (71)$$

and ΔQ values is chosen to make the total mass flow rate constant, i.e.

$$\Delta Q = \frac{M - M^*}{\sum_{all\ P} J\rho f_P} \quad (72)$$

in which "M" is the exact mass-flow rate known from the inlet conditions.

## 7. OUTLINE OF THE SOLUTION PROCEDURE

(i) Compute the coefficients for the axial momentum equation using the best available velocities and using a guessed pressure-gradient. Solve the axial momentum-equation for a tentative axial-velocity, $w^*$,

(ii) Solve for the factor "f" and calculate "ΔQ",

(iii) Calculate the corrected axial-velocity field, $w$ and the corrected pressure-gradient in the axial direction using the "$f$" and the "ΔQ" parameters. Proceed to perform an inner iteration for $w$.

(iv) Using the best available velocities, compute the coefficients for the "u" and "v" momentum equations,

(v) Compute the pseudo velocities, û and v̂ and the corresponding contravariant components $\hat{U}$ and $\hat{V}$ using the relevant relations,

(vi) Solve the Poisson-like equation for pressure, P. in which $\hat{U}$ and $\hat{V}$ are used.

(vii) Treating this pressure-field as $P^*$, solve transverse momentum equations for $u^*$ and $v^*$,

(viii) Calculate the corresponding $U^*$ and $V^*$ from the relevant equations,

(ix) Solve the Poisson-like equation for pressure-correction, P′, in which $U^*$ and $V^*$ are used,

(x) Correct $U^*$ and $V^*$ velocities using P′ solution to obtain "$U$" and "$V$" components that conserve mass and obtain the other components of "$U$" and "$V$" velocities by interpolation,

(xi) Compute the physical velocities, "$u$" and "$v$" from the latter contravariant velocities using the relevant equations.

(xii) Solve the energy equation,

(xiii) Solve the reactant continuity equation.

With the new velocity field, temperature and mass-fraction values obtained above return to step (i) and iterate up to convergence.

## 8. RESULTS AND DISCUSSION

**Fluid Flow** Numerical results are presented in Figures 1 to 5. The specific geometries selected for this analysis are as flows:

- square duct
- equilateral triangular duct
- trapezoidal duct (acute-angle = 60˚, one side twice the other)
- pentagonal duct (each angle = 108˚)

All the above ducts are selected on the basis of the same equivalent diameters. Consequently, the same value of the relaxation factor is applied to all the geometries corresponding to each discretization equation. It is believed that this scheme is valid if

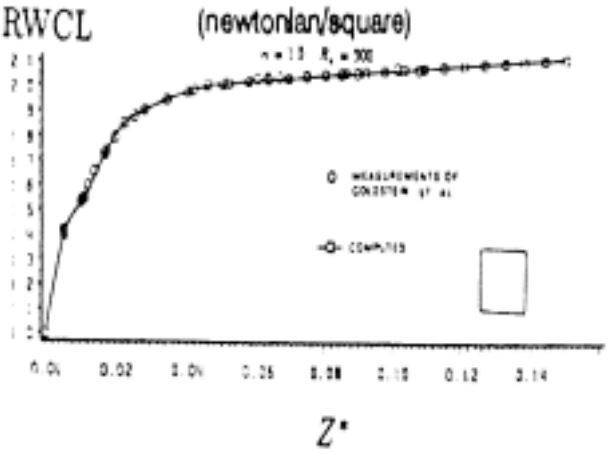


**Figure 1.** Centerline velocity development.

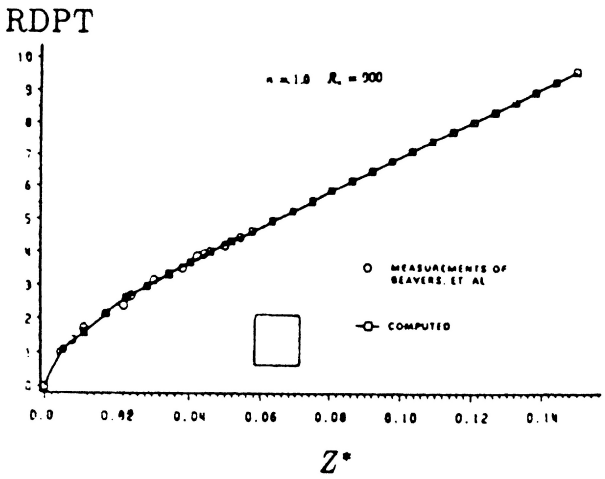


**Figure 2.** D.L. pressure-drop vs D.L. axial- distance.

**TABLE 1. Comparison of Theoretical and Predicted Results.**

| $(\frac{w_{cl}}{\overline{w}})$@ F.D. | Square Duct | Circular Duct |
|---|---|---|
| Exact | 2.096 | 2.00 |
| 21×21 | 2.110 | 1.99 |
| Error | -0.67% | 0.50% |

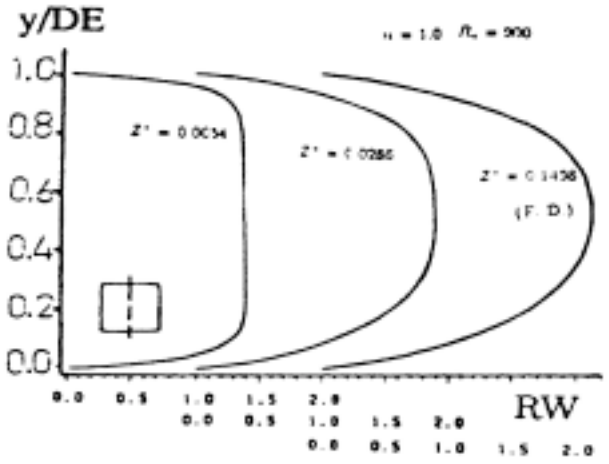


**Figure 3.** Development of axial velocity profile.

the geometries selected do not involve oddity. For a pictorial representation of this concept, one may refer to Bejan [24] for a scale drawing of the duct sizes for some geometry having the same equivalent diameter. The inlet Reynolds number values applied for the Newtonian fluid was 900 and that for the non-Newtonian case was 128 respectively. The problem is solved for constant-property fluid and the fluid is considered isothermal in the transverse direction due to which the buoyancy effect is ignored. For the sake of numerical accuracy and computational economy the mesh size selected was 21 × 21 over the transverse plane. The typical CPU time was about 3 minutes for one run on IBM ESA9000 machine (mainframe).

The Newtonian case was solved with an axial step size of 0.160 m for which 26 marching stations were required in the axial direction to converge to the fully developed flow condition. The predicted results for the centerline velocity development, axial pressure gradient and axial velocity profiles on the central plane are presented in Figures 1 to 3 for square ducts. The axial velocity results show an excellent gradual development as expected. Within the numerical accuracy, there is close agreement between the ultimate centerline velocity results and their corresponding theoretical values examined for the square and circular ducts. The computed result for the square duct centerline velocity $(\frac{w_{cl}}{\overline{w}})$ is 2.110 versus the theoretical value of 2.096 at the fully developed condition where the relative deviation between two successive values of $\frac{w_{cl}}{\overline{w}}$ only 0.24%. The computed result for the circular duct centerline velocity $(\frac{w_{cl}}{\overline{w}})$ is 1.99 versus the theoretical value of 2.00. These results provide a measure of accuracy of the grid size selected as indicated in Table 1.

Also the results obtained in the present analysis for Newtonian fluids in square ducts exhibit excellent agreement with the experimental measurements of Goldstein et al. [25] for centerline velocity development and those of Beavers et al. [26] for pressure-drop values (see Figures. 1 and 2).

About 5 iterations were required to obtain converged solution over each transversed plane. The convergence criterion was set on the basis of the residual values defined as follows:

(i). the residual of the momentum equations, that is, the remainder of these equations when the results are substituted for the velocities into these equations. In general $R = \sum a_{nb}\varphi_{nb} + b - a_P\varphi_P$ and R will be zero when the discretization equation is satisfied [11]

(ii). the residual of velocities, that is. the difference in velocity values between two successive iterations.

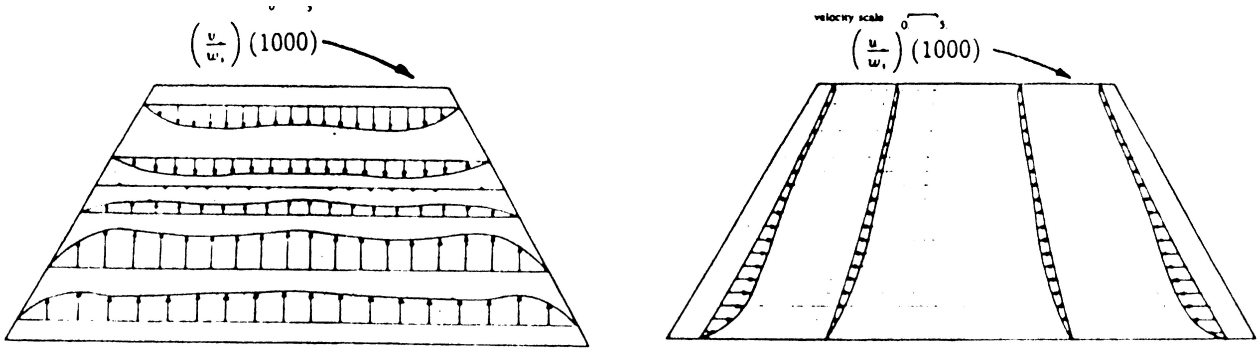


**Figure 4.** Secondary flow velocity profiles for a trapezoidal duct, Newtonian fluids Re = 900, $(z/D_h)/Re = 0.0054$.

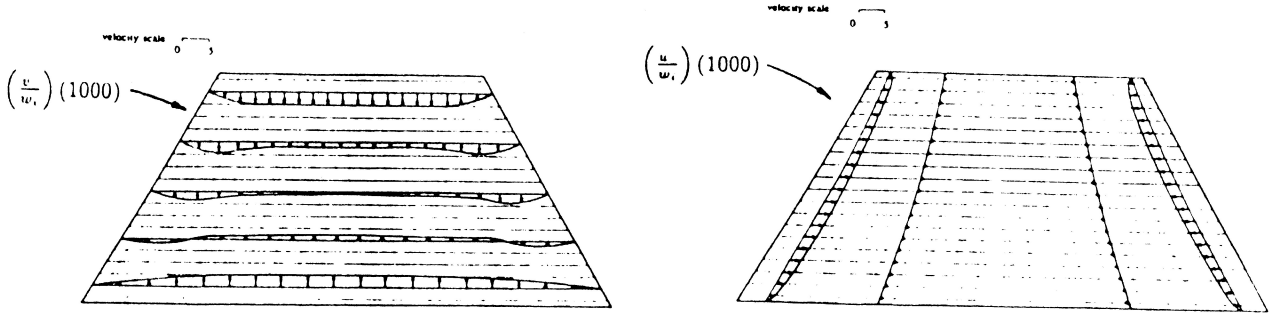


**Figure 5.** Secondary flow velocity profiles for a trapezoidal duct, non-Newtonian fluids (n = 0.5), Re = 128, $(z/D_h)/Re = 0.0115$.

**TABLE 2. Residual Values (Fluid-Flow).**

| Geometries | Momentum-equation Residual | | Velocity Residual | |
|---|---|---|---|---|
| | Transverse | Axial | Transverse | Axial |
| Square | $0.12\times10^{-6}$ | $0.21\times10^{-10}$ | $0.34\times10^{-6}$ | $-0.35\times10^{-5}$ |
| Triangular | $0.26\times10^{-6}$ | $0.98\times10^{-10}$ | $0.60\times10^{-6}$ | $-0.44\times10^{-5}$ |
| Trapezodial | $0.20\times10^{-6}$ | $0.36\times10^{-10}$ | $0.40\times10^{-6}$ | $-0.32\times10^{-5}$ |
| Pentagonal | $0.18\times10^{-6}$ | $0.52\times10^{-10}$ | $0.44\times10^{-6}$ | $-0.35\times10^{-5}$ |

Table 2 shows the residual values of momentum equations and velocities at the fully developed condition.

It should be noted that the numerical solution procedure, which was developed and implemented in this study, did not show any convergence problems.

The non-Newtonian analysis is for a polystyrene solution with a power-law index of n = 0.5 and Reynolds number value of 128 at inlet. The axial-step size selected was 0.05 m. The axial velocity development shows a plug-flow behavior at all four arbitrary cross-sectional ducts chosen, although the triangular duct shows a slight delay in the development to a plug flow velocity profile. The plug flow behavior observed for the non-Newtonian case was previously predicted by Husain and Hamielec [27].

Husain and Hamielec [27] in their analytical studies of tubular styrene polymerization. The non-

**TABLE 3. Comparison of Limiting Nusselt Numbers.**

| | Square | Rectangular(2/1) | Rectangular(3/2) | Equilateral Triangular | Circular |
|---|---|---|---|---|---|
| Clark and Kays | 2.890 | 3.390 | - | - | - |
| Dennis et al. | 2.980 | 3.390 | 3.120 | - | - |
| Shah and London | 2.976 | 3.391 | 3.117 | - | - |
| Schmidt | 2.970 | 3.383 | 3.121 | - | - |
| Javeri | 2.981 | 3.393 | - | - | - |
| Lyczkowski et al. | 2.975 | 3.395 | 3.117 | - | - |
| Kays and Crawford | 2.980 | 3.390 | - | 2.350 | 3.658 |
| Wibulswas | - | - | - | 2.570 | - |
| This Study | 2.980 | 3.363 | 3.118 | 2.598 | 3.603 |

**TABLE 4. Residual Values (Heat-Transfer).**

| Geometry | Energy-equation Residual | Enthalpy Residual |
|---|---|---|
| Square | $0.303\times10^{-7}$ | $-0.275\times10^{-4}$ |
| Triangular | $0.160\times10^{-6}$ | $-0.270\times10^{-4}$ |
| Trapezoidal | $0.533\times10^{-7}$ | $-0.270\times10^{-4}$ |
| Pentagonal | $0.694\times10^{-7}$ | $-0.385\times10^{-4}$ |
| Rectangular(2/1) | $0.224\times10^{-7}$ | $-0.357\times10^{-4}$ |
| Rectangular(3/2) | $0.262\times10^{-7}$ | $-0.315\times10^{-4}$ |
| Circular | $0.105\times10^{-6}$ | $-0.501\times10^{-4}$ |

Newtonian case applied to circular ducts in this analysis also showed a plug flow behavior. It is, however, worthwhile to mention that specific non-Newtonian cases should be investigated separately due to the wide range of viscosities involved and the power- law indices.

The solution procedure showed a lower critical limit of axial step size, $\Delta\sigma = 0.01$ m, at which u and v components of velocity field (secondary flow) could not be obtained in conjunction with the w component (primary flow). An upper limit was also observed for the values of $\Delta\sigma$ selected beyond the value mentioned above for both Newtonian and non-Newtonian cases.

The transverse velocity components, u and v, supply the fluid that permit axial flow development, the highest value of which occur near the entrance where the most rapid arrangement of the axial velocity takes place. In laminar flow, due to the very small components of transverse velocities, the secondary flow has a small effect on the primary flow and the axial pressure-gradient [10,16]. The results of secondary flow analysis, for trapezoidal ducts, for Newtonian and non-Newtonian cases at one axial location, are presented in Figures 4 and 5. Comparing the corresponding $z/D_h$ values, it is observed that the axial location for non- Newtonian case is closer to the entrance than for the Newtonian case. The secondary flow is away from the walls towards the

**TABLE 5. Husain and Hamielec [27], 1976, Simulation Results.**

| Length Z(cm) | Conversion wt% | Molecular- Weight $M_n \times 10^{-5}$ | $M_n \times 10^{-5}$ | Polydispersity $\frac{M_w}{M_n}$ |
|---|---|---|---|---|
| 100 | 1.26 | 4.16 | 7.34 | 1.77 |
| 300 | 3.95 | 4.04 | 7.16 | 1.77 |
| 500 | 6.62 | 3.96 | 7.08 | 1.78 |

**TABLE 6. Present Work Simulation Results.**
**Number of Stations Selected in Axial Direction: 5.**

| Length Z(cm) | Conversion wt% | Molecular- Weight $M_n \times 10^{-5}$ | $M_n \times 10^{-5}$ | Polydispersity $\frac{M_w}{M_n}$ | Total $\Delta P(Pa)$ |
|---|---|---|---|---|---|
| 100 | 1.38 | 4.22 | 7.43 | 1.76 | 0.037 |
| 300 | 4.14 | 4.75 | 8.68 | 1.83 | 0.40 |
| 500 | 6.74 | 4.52 | 8.20 | 1.81 | 1.46 |

**TABLE 7. Present Work Simulation Results.**
**Number of Stations Selected in Axial Direction: 10.**

| Length Z(cm) | Conversion wt% | Molecular- Weight $M_n \times 10^{-5}$ | $M_n \times 10^{-5}$ | Polydispersity $\frac{M_w}{M_n}$ | Total $\Delta P(Pa)$ |
|---|---|---|---|---|---|
| 100 | 1.37 | 5.09 | 9.33 | 1.83 | 0.06 |
| 300 | 3.95 | 4.48 | 8.08 | 1.80 | 0.48 |
| 500 | 6.34 | 4.40 | 7.87 | 1.79 | 1.74 |

intermediate sections at which it is reversed in direction for all the geometries. The order of magnitude of the secondary flow velocities for square ducts obtained in this work conforms to the results illustrated by Briley [10]. Comparing Newtonian and non-Newtonian secondary-flow results, it is observed that the results of Newtonian case are relatively higher than the results of non-Newtonian case. The reason for this difference is attributed to the primary velocity profile patterns of the two cases, that is, tending to parabolic for Newtonian and plug-flow for non-Newtonian cases.

**Heat Transfer** The limiting Nusselt number ($N_{uT}$) for square, rectangular, triangular and circular ducts obtained in this study are compared with analytical and numerical results of other investigators in Table 3. The analysis was made for $P_r$ = 6.78 and constant wall temperature case. These results confirm the validity of the model and computer code for heat transfer in this study.

This study was performed on the basis of the same equivalent diameters. The mesh size selected was 21 × 21 over the transverse-plane as before. The problem was solved for an axial step size of 0.276 m for which 250 marching stations were

**TABLE 8. Residual Values(Mass Transfer).**

| Species-continuity equation residual | Mass-fraction residual |
|---|---|
| $0.2\times10^{-7}$ | $0.2\times10^{-2}$ |

**TABLE 9. Simulation Results of Styrene Polymerization at Reactor Exit.**

| No. | Geometry | WPA (wt%) | $\overline{M}_n$ $(\frac{kg}{kgmol})$ | $\overline{M}_w$ $(\frac{kg}{kgmol})$ | Polydispersity $\frac{\overline{M}_w}{\overline{M}_n}$ | Bulk-temp (˚C) | Total DP (Pa) |
|---|---|---|---|---|---|---|---|
| 1 | Circular | 6.74 | 452460 | 819590 | 1.81 | 102.3 | 1.46 |
| 2 | Square | 6.74 | 452910 | 820240 | 1.81 | 102.2 | 1.88 |
| 3 | Triangular | 6.38 | 453450 | 820660 | 1.81 | 101.9 | 2.70 |
| 4 | Trapezoidal | 6.33 | 454100 | 822100 | 1.81 | 101.9 | 2.57 |
| 5 | Pentagonal | 6.63 | 453810 | 822110 | 1.81 | 102.1 | 2.28 |
| 6 | Hexagonal | 6.74 | 452940 | 820450 | 1.81 | 102.3 | 1.69 |
| 7 | Rectangular(AR=1.5) | 6.70 | 453784 | 821697 | 1.81 | 102.0 | 1.91 |
| 8 | Rectangular(AR=2.0) | 6.63 | 455120 | 823870 | 1.81 | 101.8 | 1.97 |

required in the axial-direction. The typical CPU time required was about 26 minutes for one run on IBM ESA9000 machine. The computations were performed for fully developed velocity and developing temperature profiles. About 5 iterations were required to obtain converged solution over each transverse plane. The convergence criteria was set on the residual values similarly defined for the Fluid-Flow study mentioned before, that is, the residuals for this study are as follows:

(i) the residual of energy equation,

(ii) the residual of enthalpy values between two successive iterations.

Table 4 shows the residual values of energy equation and enthalpy values at the converged solution.

**Mass Transfer with Chemical Reaction** The thermal polymerization of styrene is selected in this study for analysis in arbitrary cross-sectional duct reactors. The validation of system modeling and computer codes for mass transfer is accomplished through comparison of the results of other investigators with the predicted results obtained by the present analysis. One typical comparison is presented in Tables 5, 6, and 7. The above results are related to the following operating data:

| | |
|---|---|
| length of tube | 500 cm |
| tube radius | 2.0cm |
| inlet velocity | 0.0695 cm/sec |
| inlet/wall temperature | 100˚ C/100˚C |

Employing the above operating data, this work was conducted for the analysis of thermal polymerization of styrene in arbitrary cross-sectional duct reactors for eight different geometries. The same mesh-size on transversed plane was used as before. Typical CPU time was about 10 minutes for the longest run on IBM ESA9000 machine. About 5 iterations were required on each transversed plane for convergence. The same convergence indicators were selected as mentioned previously in Fluid-Flow and Heat-Transfer sections. Refer to Table 8 in this respect.

The basis for computations in all the reactors bearing different geometries in their cross sections and the same length is the same residence-time in the reactors or the same cross sectional area, while the same uniform velocity is maintained at inlet of each reactor. Refer to Table 9 for the simulation results of styrene polymerization in eight different geometries corresponding to the above-mentioned operating conditions.

## 9. CONCLUSIONS

This paper demonstrates the application of a non-orthogonal boundary-fitted coordinate transformation method to the solution of 3D parabolized conservation equations of reacting laminar flow in various ducts of non-circular cross-sections. The solution procedure has been modified to handle non-orthogonal boundary-fitted method and non-Newtonian fluids. The results of validation of system model and computer codes are excellent.

## 10. NOMENCLATURE

| | |
|---|---|
| A, a | coefficient in discretization equation |
| AR, ar | aspect ratio |
| B, b | constant term in discretization equation |
| $C_P$ | specific heat |
| DP | pressure drop |
| DE, $D_h$ | equivalent or hydraulic diameter |
| $D_A$ | mass diffusivity of A |
| D.L. | dimensionless |
| f | defined by Equation (68) |
| F. D. | fully-developed |
| g | acceleration due to gravity |
| h | enthalpy (h = $C_P$T) |
| J | Jacobian of transformation |
| k | thermal conductivity |
| m | mass fraction |
| M | apparent viscosity for a power-law fluid |
| M | mass flow rate |
| $\overline{M}_w$ | cup-averaged weight average molecular-weight |
| $\overline{M}_n$ | cup-averaged number average molecular-weight |
| n | power-law index |
| n | unit normal vector |
| $N_{uT}$ | limiting Nusselt number |
| P | pressure |
| $P'$ | pressure correction |
| $P_0$ | static pressure at inlet |
| $\overline{P}$ | mean viscous pressure |
| q | heat flux |
| Q | defined by Equation (68) |
| RDPT | $(P_0 - \overline{P})/(\frac{1}{2}\rho w_0^2)$ |
| R | residual of discretization equation |
| $R_A$ | mass rate of consumption of reactant "A" due to chemical reaction |
| $R_e$ | Reynolds number $(R_e = \frac{\rho D_h^n \overline{w}^{2-n}}{\mu})$ |
| RW | axial velocity ratio $\left(\frac{w}{\overline{w}}\right)$ |
| RWCL | centerline velocity ratio $\left(\frac{w_{cl}}{\overline{w}}\right)$ |
| SC | constant part of linearized source term |
| SP | coefficient of the dependent variable in the linearized source term |
| $\overline{w}$ | mean axial velocity |
| $w_{cl}$ | centerline velocity |
| $w_0$ | inlet velocity |
| WPA | polymer average weight fraction |
| $u,v,w$ | velocity components in the Cartesian system |
| $\hat{u},\hat{v},\hat{w}$ | pseudovelocity components |
| $\hat{U},\hat{V},\hat{W}$ | pseudovelocity components (contravariant) |
| $u^*,v^*,w^*$ | tentative velocity field |
| $U^*,V^*,W^*$ | tentative contravariant velocity field |
| x,y,z | Cartesian coordinate system |
| Z | duct length |
| $Z^*$ | dimensionless axial-distance, $Z^* = \frac{z}{D_h.R_e(local)}$ |

### Greek Letters

| | |
|---|---|
| α | relaxation factor |
| α, β, γ | coordinate transformation coefficients |
| $\xi,\eta,\sigma$ | axes of curvilinear coordinate |
| $\mu$ | consistency index (for power-law fluids) and viscosity (for Newtonian fluids) |
| $\rho$ | density |
| $\rho_a$ | arithmetic mean density for duct cross-section |
| $\tau_{ij}$ | stress-tensor |
| $\Delta H$ | heat of reaction |

| | |
|---|---|
| $\Delta_{ij}$ | rate of deformation tensor |
| $\Delta P$ | pressure-drop in the duct |
| $\Delta V$ | change in volume |
| $\varphi$ | general dependent variable |
| $\Phi$ | viscous dissipation function |

## Superscripts

| | |
|---|---|
| ^ | refers to transformed quantities, except for velocities |

## Subscripts

| | |
|---|---|
| nb | general neighbor grid point |
| P | central grid point under consideration |
| U | upstream plane |
| D | downstream plane |
| E ,W, N, S | nodes neighboring to P |
| NE, NW | nodes neighboring to P |
| SE, SW | nodes neighboring to P |

## Special Symbols

| | |
|---|---|
| L[ ] | finite-difference approximation of the quantity in brackets |

## 11. REFERENCES


1. Thompson, J. F., "Three-Dimensional Grid Generation for Complex Configuration Recent Progress", AGARD 309, North Atlantic Treaty Organization, (1988).
2. Ramanathan, S. and Kumar R., "Comparison of Boundary-Fitted Coordinates with Finite-Element Approach for Solution of Conduction Problems", ***Numerical Heat Transfer,*** Vol. 14, (1988), 187-211.
3. Chu, W. H., "Development of a General Finite Difference Approximation for a General Domain", ***J. Comp. Physics,*** Vol. 8, (1971), 392-408.
4. Thames, F. C., Thompson, J. F., Mastin, C. W. and Walker, R. L., "Numerical Solutions for Viscous and Potential Flow about Arbitrary Two-Dimensional Bodies Using Body-Fitted Coordinate System", ***J. Comp. Physics,*** Vol. 24, (1977), 245-273.
5. Thompson, J. F., Thames, F. C. and Mastin, C. W., "TOMCAT - A Code for Numerical Generation of Boundary Fitted Curvilinear Coordinate Systems on Fields Containing any Number of Arbitrary Two-Dimensional Bodies", ***J. Comp. Physics,*** Vol. 24, (1977), 274-302.
6. Thompson, J. F., Thames, F. C. and Mastin, C. W., "Boundary-Fitted Curvilinear Coordinate Systems for Solution of Partial Differential Equations on Fields Containing any Number of Arbitrary Two-Dimensional Bodies", ***Report CR-2729,*** NASA Langley Research Centre, (1977).
7. Thompson, J. F., Warsi, U. A. and Mastin, C. W., "Boundary-Fitted Coordinate Systems for Numerical Solution of Partial Differential Equations A Review", ***J. Comp. Physics,*** Vol. 47, (1982), 1-108.
8. Caretto, L. S., Curr, R. M. and Spalding, D. B., "Compt. Meth. Appl. Mech. and Engr.", Vol. 1, (1973), 39.
9. Patankar, S. V. and Spalding, D. B., "A Calculation Procedure for Heat, Mass and Momentum Transfer in Three-Dimensional Parabolic Flows", ***International Journal of Heat and Mass Transfer,*** Vol. 15, (1972), 1787-1806.
10. Briley, W. R, "Numerical Method for Predicting Three-Dimensional Steady Viscous Flow in Ducts", ***Journal of Computational Physics,*** Vol. 14, (1974), 8-28.
11. Patankar, S. V, "Numerical Heat Transfer and Fluid Flow", Hemisphere Publishing Corporation., N. Y., (1980).
12. Hadjisophocleous, G. V., Sousa, A. C. M. and Venart, J. E. S., "Prediction of Transient Natural Convection in Enclosures of Arbitrary Geometry Using a Nonorthogonal Numerical Model", ***Numerical Heat Transfer,*** Vol. 13, (1988), 373-392.
13. Shyy, W., Tong, S. S. and Correa, S. M., "Numerical Recirculating Flow Calculation Using a Body-Fitted Coordinate System", ***Numerical Heat Transfer***, Vol. 8, (1985), 99-113.
14. Braaten, M. and Shyy, W., "A Study of Recirculating Flow Computation Using Body-Fitted Coordinates: Consistency Aspects and Mesh Skewness", ***Numerical Heat Transfer,*** Vol. 9, (1988), 559-574.
15. Maliska, C. R., "A Solution Method for Three-Dimensional Parabolic Fluid Flow Problems in Nonorthogonal Coordinates", Ph. D. Thesis, University of Waterloo, Canada, (1981).
16. Maliska, C. R. and Raithby, G. D., "A Method for Computing Three Dimensional Flows Using Non-Orthogonal Boundary-Fitted Coordinates", ***International Journal for Numerical Methods in Fluids,*** Vol. 4, (1984), 519-537.
17. Bird, R. B., Stewart, W. E. and Lightfoot, E. N., "Transport Phenomena", John Wiley and Sons, N. Y., (1960).
18. Skelland, A. H. P., "Non-Newtonian Flow and Heat-Transfer", John Wiley and Sons, N. Y., (1967).
19. Lawal, A., "Laminar Flow and Heat-Transfer to Variable Property Power Law Fluids in Ducts of Arbitrary But Uniform Cross-Section", Ph. D. Thesis, McGill University, (1985).
20. Kakac, S., Shah, R. K. and Aung, W., "Handbook of Single-Phase Convective Heat Transfer", John Wiley and Sons, N. Y., (1987).
21. Allen, P. H. G., "Heat and Mass Transfer by Combined Forced and Natural Convection", ***The Institution of Mechanical Engineers***, (1972).
22. Ostrach, S., "Laminar Natural-Convection Flow and Heat Transfer of Fluids With and Without Heat Sources in Channels with Constant Wall Temperatures", ***NACA Technical Note 2863,*** (1952).
23. Raithby, G. D. and Schneider, G. E., "Numerical Solution of Problems in Incompressible Fluid Flow: Treatment of

the Velocity-Pressure Coupling", ***Numerical Heat Transfer***, Vol. 2, (1979), 417-440.
24. Bejan, A., "Convection Heat Transfer", John Wiley and Sons, N. Y., (1984).
25. Goldstein, R. G. and Kreid, D. K., "Measurement of Laminar Flow Development in a Square Duct Using a Laser-Doppler Flowmeter", ***J. Appl. Mech.,*** Vol. 34, (1967), 813-818.
26. Beavers, G. S., Sparrow, E. M. and Magnuson, "Experiments on Hydrodynamically Developing Flow in Rectangular Ducts of Arbitrary Aspect Ratio", ***International Journal of Heat and Mass Transfer,*** Vol. 13, (1970), 689-702.
27. Husain, A. and Hamielec, A. E., "Bulk Thermal Polymerization of Styrene in a Tubular Reactor - a Computer Study", ***AIChE Symposium Series,*** Vol. 72, No. 160, (1976), 112-127.
28. Lyczkowski, R. W., Solbrig, C. W. and Gidaspow, D., "Forced Convection Heat Transfer in Rectangular Duct", ***Nuclear Engineering Design***, Vol. 67, (1981), 357-378.
29. Dennis, S. C. R., Mercer, A. M. and Poots, G., "Forced Heat Convection in Laminar Flow Through Rectangular Ducts", ***Q. Appl. Math.***, Vol. 17, (1959), 285-297.
30. Kays, W. M. and Crawford, M. E., "Convective Heat and Mass Transfer", 2nd Ed., McGraw-Hill, N. Y., (1980).
31. Wibulswas, P., "Laminar Flow Heat Transfer in Non-Circular Ducts", Ph. D. Thesis, London University, London, U.K., (1966).